Electrodeposition of Au−Cd Alloy Nanostructures on Au(111)

Marcus D. Lay and John L. Stickney*

Contribution from the Department of Chemistry, University of Georgia, Athens, Georgia 30602

Received September 30, 2002 ; E-mail: Stickney@sunchem.chem.uga.edu

Abstract: This report concerns an in-situ scanning tunneling microscopy study of the initial stages in the formation of a Au−Cd alloy on the Au(111) herringbone reconstruction. Although Au−Cd nanoclusters of alloy have been observed in sulfate electrolyte by this group, alloy "nanowires" were observed to form preferentially in the hcp regions between the sets of "soliton" walls of the reconstruction only in the presence of chloride. The nanowires were formed at −0.55 V versus 3 M Ag/AgCl, corresponding to Cd underpotential deposition (upd). Upd is electrodeposition at a potential prior to that needed to deposit the bulk element.

Introduction

The formation and characterization of nanostructures is a central theme in materials research. Of particular interest is the use of nanometer scale templates to direct synthesis. Such efforts include the patterning of SAMs with contact printing,[1,2] and the use of track etched membranes,[3] anodized aluminum membranes,[4−6] and surface assembled micelle-like structures.[7,8] This report concerns the use of the Au(111) herringbone reconstruction as a template for the electrodeposition of arrays of Au−Cd alloy nanostructures. The formation of arrays of nanoparticles and wires of compound semiconductors is suggested. That is, formation of compounds such as CdTe, CdSe, and CdS, by the subsequent deposition of chalcogenides, using electrochemical atomic layer epitaxy (EC-ALE),[9,10] may be possible.

The herringbone reconstruction lowers the surface free energy via a uniaxial compression, resulting in 23 surface Au atoms occupying the space of 22, and forming an array of "soliton" walls (characterized by surface atoms sitting in bridge sites on the second Au layer). The walls separate thinner hcp regions from wider fcc regions.[11,12] The herringbone reconstruction has been observed by scanning tunneling microscopy (STM) in a vacuum,[13,14] and in ambient[15] and aqueous solution.[16] The morphology of the Au walls has been shown to depend strongly on annealing and cooling conditions in the case of Au(100).[17]

It has been observed that Fe,[18] Ni,[19,20] and Co[21] deposit initially at elbows in the soliton walls of the Au(111) reconstruction. Strain induced by lattice dislocations at these elbows was initially proposed to account for this nucleation;[18−21] however, recently, a place exchange mechanism has been suggested in the case of Ni electrodeposition.[22] Pb and Ru electrodeposits on Au have been found to decorate the fcc regions of the reconstruction with 2 nm randomized clusters.[23,24]

Cd is known to alloy with Au at potentials prior to bulk Cd deposition,[25,26] in the upd region.[27] It has also been proposed that Cd upd on Au(100) occurs via a process wherein a thin alloy "skin", encompassing the first few substrate atomic layers, is initially formed; its thickness is directly related to the distance from the pzc. Further alloying with Au occurs at a considerably slower pace as Cd atoms diffuse into the bulk.[28] Diffusion

(1) Kumar, A.; Biebuyck, H. A.; Whitesides, G. M. *Langmuir* **1994**, *10*, 1498−1511.
(2) Qin, D.; Xia, Y. N.; Rogers, J. A.; Jackman, R. J.; Zhao, X. M.; Whitesides, G. M. *Microsystem Technology in Chemistry and Life Science*; Becker, H., Manz, A., Eds.; Springer−Verlag, Incorporated: New York, 1998; Vol. 194, pp 1−20.
(3) Kuo, T. C.; Sloan, L. A.; Sweedler, J. V.; Bohn, P. W. *Langmuir* **2001**, *17*, 6298−6303.
(4) Masuda, H.; Fukuda, K. *Science* **1995**, *268*, 1466−1468.
(5) Sun, M.; Zangari, G.; Shamsuzzoha, M.; Metzger, R. M. *Appl. Phys. Lett.* **2001**, *78*, 2964−2966.
(6) Possin, G. E. *Rev. Sci. Instrum.* **1970**, *41*, 772−774.
(7) Kresge, C. T.; Leonowicz, M. E.; Roth, W. J.; Vartuli, J. C.; Beck, J. S. *Nature* **1992**, *359*, 710−712.
(8) Attard, G. S.; Goltner, C. G.; Corker, J. M.; Henke, S.; Templer, R. *Angew. Chem., Int. Ed. Engl.* **1997**, *36*, 1316−1317.
(9) Gregory, B. W.; Stickney, J. L. *J. Electroanal. Chem.* **1991**, *300*, 543−561.
(10) Stickney, J. L.; Wade, T. L.; Flowers, B. H., Jr.; Vaidyanathan, R.; Happek, U. In *Encyclopedia of Electrochemistry*; Gileadi, E., Urbakh, M., Eds.; Marcel Dekker: New York, 2002; Vol. in press.
(11) J. V., B.; H., B.; G., E.; R. J., B. *Phys. Rev. B* **1990**, *42*, 9307.
(12) Bach, C. E.; Giesen, M.; Ibach, H.; Einstein, T. L. *Phys. Rev. Lett.* **1997**, *78*, 4225−4228.
(13) Barth, J. V.; Brune, H.; Ertl, G.; Behm, R. J. *Phys. Rev. B* **1990**, *42*, 9307−9318.
(14) Woll, C.; Chiang, S.; Wilson, R. J.; P. H., L. *Phys. Rev. B* **1989**, *39*, 7988−7991.
(15) Mizutani, W.; Ohi, A.; Motomatsu, M.; Tokumoto, H. *Appl. Surf. Sci.* **1995**, *87−8*, 398−404.
(16) Tao, N. J.; Lindsay, S. M. *J. Appl. Phys.* **1991**, *70*, 5141−5143.
(17) Batina, N.; Dakkouri, A. S.; Kolb, D. M. *J. Electroanal. Chem.* **1994**, *370*, 87−94.
(18) Stroscio, J. A.; Pierce, D. T.; Dragoset, R. A.; First, P. N. *J. Vac. Sci. Technol., A* **1992**, *10*, 1981−1985.
(19) Chambliss, D. D.; Wilson, R. J.; Chiang, S. *J. Vac. Sci. Technol.* **1991**, *9*, 933−937.
(20) Chambliss, D. D.; Wilson, R. J.; Chiang, S. *Phys. Rev. Lett.* **1991**, *66*, 1721−1724.
(21) Voigtlander, B.; Meyer, G.; Amer, N. M. *Phys. Rev. B* **1991**, *44*, 10354−10357.
(22) Meyer, J. A.; Baikie, I. D.; Kopatzki, E.; Behm, R. J. *Surf. Sci.* **1996**, *365*, L647−L651.
(23) Tao, N. J. P., J.; Li, Y.; Oden, P. I.; DeRose, J. A.; Lindsay, S. M. *Surf. Sci. Lett.* **1992**, *271*, L338−L344.
(24) Strbac, S.; Magnussen, O. M.; Behm, R. J. *Phys. Rev. Lett.* **1999**, *83*, 3246−3249.
(25) Vidu, R.; Hira, N.; Hara, S. *Phys. Chem. Chem. Phys.* **2001**, *3*, 3320−3324.
(26) Inzelt, G.; Horanyi, G. *J. Electroanal. Chem.* **2000**, *491*, 111−116.
(27) Leiva, E. *Electrochim. Acta* **1996**, *41*, 2185−2206.
(28) Vidu, R.; Hirai, N.; Hara, S. *Phys. Chem. Chem. Phys.* **2001**, *3*, 3320−3324.
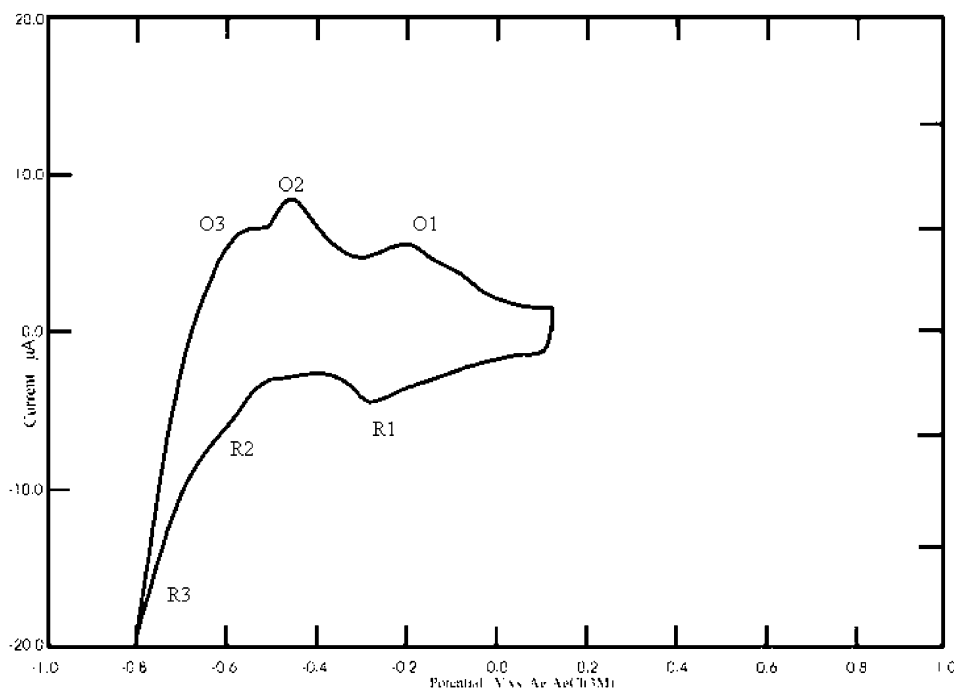
Figure 1. Cyclic voltammogram of a Au(111) single crystal in 0.20 mM CdCl$_2$ + 1 mM HCl (pH 3). Scan rate = 0.005 V/s.

coefficients for the two processes seemed to indicate a transition from a turnover to a solid-state diffusion mechanism.

The importance of electrolyte coadsorption in Cd electrodeposition has been clearly shown by Gewirth et al.[29,30] Cd electrodeposition from solutions containing sulfate, chloride, acetate, and perchlorate has been studied in this group. Alloy formation has also been observed in sulfate-containing solutions, although the influence of the soliton walls on Au−Cd alloy morphology was most pronounced in chloride-containing electrolyte. Chloride ions have been shown to increase the mobility of surface Au atoms[31] and to promote the alloying of Cu with Au.[32]

Experimental Section

For cyclic voltammetry, a 99.999% pure Au(111) single crystal (MaTecK GmbH) was used. The substrates for in-situ STM were composed of gold evaporated onto borosilicate glass slides. The Au-(111) single crystal and Au on glass substrates were cleaned in hot nitric acid for 30 min and were then annealed in a hydrogen flame for 7 min. This procedure routinely yielded large atomically flat terraces on which the gold herringbone reconstruction was visible.

Cd deposition solutions were composed of 0.20 mM CdCl$_2$ + 1.0 mM HCl, prepared with ultrapure water (>18.1 MΩ) and analytical grade reagents. In-situ scanning tunneling microscopy (STM) studies were carried out in constant current mode (height mode), using a Nanoscope III (Digital Instruments, Santa Barbara, CA). The instrument was calibrated by imaging HOPG in air. For all imaging, tips were formed from polycrystalline tungsten wire (diameter = 0.25 mm), etched at 12 VAC in fresh 1 M KOH. To reduce Faradaic currents at the tip/electrolyte interface, tips were coated with hot glue gun glue (Kmart), leaving only the apex exposed. The electrochemical STM cell has been described previously.[33] The entire setup, including the cell

and scanning head, was isolated from ambient by fitting a Plexiglas hat on top of the microscope, and maintaining a positive pressure of high purity Ar on the system. All potentials were referenced to a 3 M Ag/AgCl reference electrode (BAS), and Au wires served as auxiliary electrodes.

Results and Discussion

The voltammetry for a Au(111) crystal in 0.2 mM CdCl$_2$ and 1 mM HCl is shown in Figure 1. Peak R1 (−0.25 V) corresponds to Cd upd. The corresponding coverage from coulometry (170 μC/cm^2) was 0.3 monolayers (ML), neglecting possible anion effects.[34] Peak R2 (−0.56 V) is a shoulder on R3, where both R2 and R3 correspond to formation of a Au−Cd alloy. On the reverse scan, oxidation peaks were numbered to correlate with the reduction features. Cd deposition at potentials negative of −0.8 V resulted in bulk Cd deposition.[35] Cyclic voltammograms to successively negative potentials (potential window opening) indicated that the anodic dissolution of Cd from the alloy was kinetically slow and was observed along with upd stripping at 0.20 V.

The image in Figure 2a was obtained at −0.4 V, after Cd upd, and clearly shows the soliton walls of the Au reconstruction; that is, Cd upd does not lift the reconstruction. This is unusual for a system where one element is chemisorbed on a reconstructed surface. An arrow marks a defect in the soliton walls (Figure 2a), which subsequently acts as a nucleation point for a 3 nm cluster at −0.50 V (Figure 2b). At −0.56 V, the Au−Cd alloy was imaged as it formed (Figure 2c).

Evident in Figure 2d is a series of atomically high nanowires, of varying length, which grew between the sets of soliton walls, preferentially in the hcp regions of the reconstructed surface. All wires followed √3 directions of the substrate atoms and were thus rotated by 120° from each other, as well as 30° from

(29) Bondos, J. C.; Gewirth, A. A.; Nuzzo, R. G. *J. Phys. Chem.* **1996**, *100*, 8617−8620.
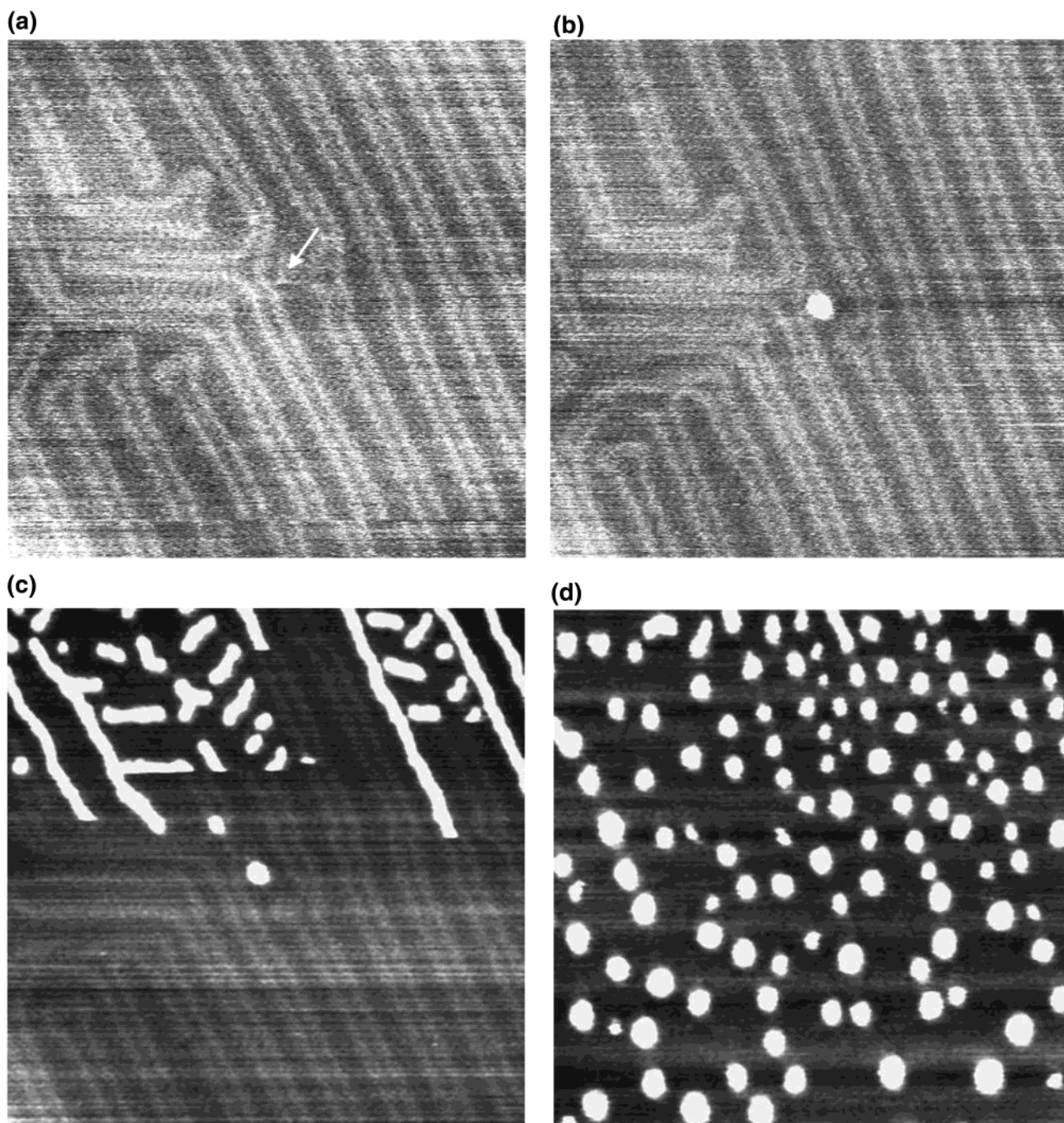(30) Hsieh, S. J.; Gewirth, A. A. *Langmuir* **2000**, *16*, 9501−9512.
(31) Weichers, J.; Twomey, T.; Kolb, D. M.; Behm, R. J. *J. Electroanal. Chem.* **1988**, *248*, 451−460.
(32) Moller, F. A.; Magnussen, O. M.; Behm, R. J. *Phys. Rev. B* **1995**, *51*, 2484−2490.
(33) Suggs, D. W.; Bard, A. J. *J. Am. Chem. Soc.* **1994**, *116*, 10725−10733.
(34) Michaelis, R.; Zei, M. S.; Zhai, R. S.; Kolb, D. M. *J. Electroanal. Chem.* **1992**, *339*, 299−310.
(35) Vidu, R.; Hara, S. *Surf. Sci.* **2000**, *452*, 229−238.

(a)

(b)

(c)

(d)

Figure 2. In-situ STM images of reconstructed Au(111), including the growth of a Au−Cd surface alloy, in 0.20 mM $CdCl_2$ + 1 mM HCl at potentials of: (a,b) −0.50, (c) −0.60, (d) −0.04 V versus Ag/AgCl. Scan size is 70 × 70 nm^2.

the rows of Au substrate atoms. Some defects in the surface appear to disturb wire growth, leading to shorter wires or nanodots, still rotated by 120° with respect to each other. It appears that at a critical distance from the pzc, the amount of Cd in the alloy phase increases to a point where these monatomic protrusions form.

Scanning positively to −0.234 V (Figure 2d) initiated dealloying, leaving a series of nanoclusters and no evidence of the soliton walls or Au reconstruction. As the wires etched, they converted into rows of circular alloy nanoclusters. As the Cd stripped from the alloy clusters, they slowly coalesced into larger, monatomic Au-rich clusters (Figure 3), with pits, characteristic of dealloying,[36] remaining. The Au surface could

then be electrochemically annealed at potentials positive of 0.10 V,[37,38] resulting in the return of the smooth Au surface, followed by the recurrence of the Au reconstruction (Figure 4).

In other experiments, involving less negative potential excursions (Figure 5a), some of the sets of soliton walls were left unfilled by the alloy and were still evident during dissolution, suggesting that wire deposition lifted the reconstruction locally. Following oxidative dissolution of the wires, pits remained only

(36) Goetting, L. B.; Huang, B. M.; Lister, T. E.; Stickney, J. L. *Electrochim. Acta* **1995**, *40*, 143−158.
(37) Wu, Y. C.; Pickering, H. W.; Gregory, D. S.; Geh, S.; Sakurai, T. *Surf. Sci.* **1991**, *246*, 468−476.
(38) Jerkiewicz, G.; Conway, B. E. *J. Chim. Phys. Phys.-Chim. Biol.* **1991**, *88*, 1381−1400.
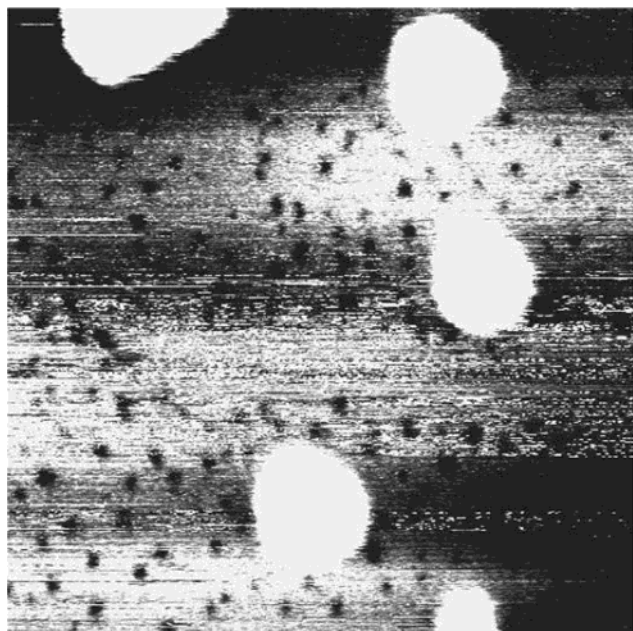
Figure 3. STM image of the Au(111) surface after dissolution of the Au–Cd surface alloy and coalescence of resulting islands. Potential = −0.038 V versus Ag/AgCl. Scan size is 70 × 70 nm^2.
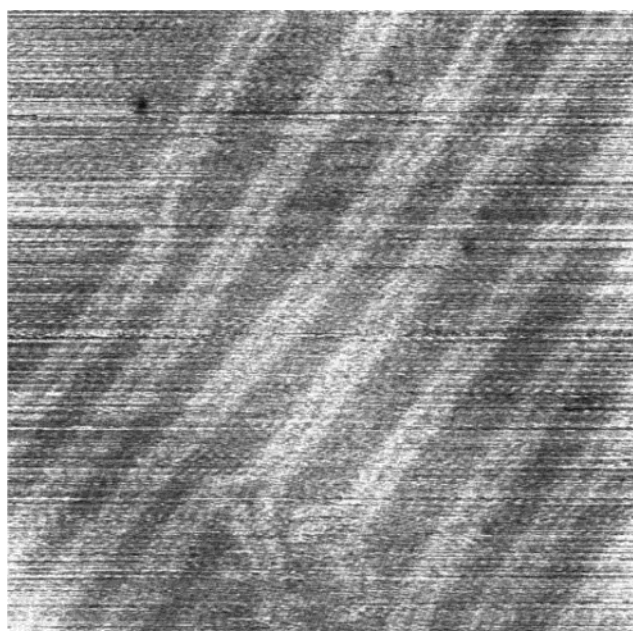
Figure 4. STM image of the return of the Au(111) reconstruction after electrochemical annealing at 0.170 V versus Ag/AgCl. Scan size is 70 × 70 nm^2.

where the wires existed (Figure 5b), indicating that the pits result from the dissolution of the alloy phase and not the upd Cd.
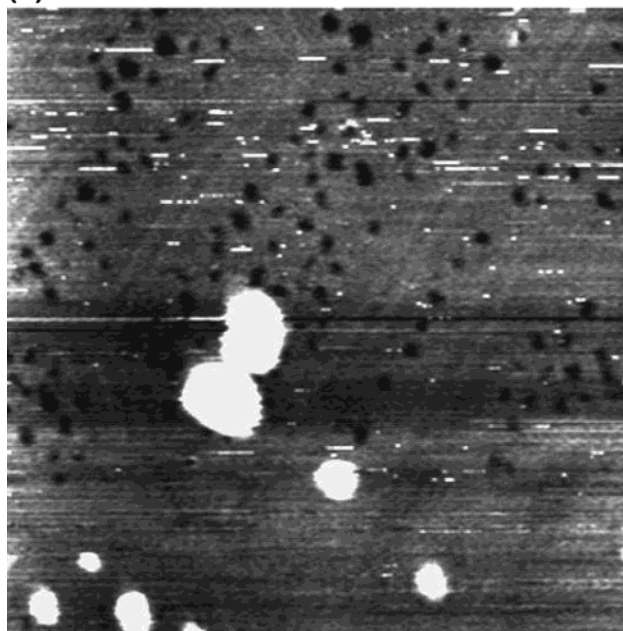
Conclusion

In conclusion, it appears that the reconstructed Au surface provides a template for the formation of Au−Cd alloy nano-

Figure 5. STM image of the Au(111) surface: (a) After the formation of the Au−Cd surface alloy at −0.498 V versus Ag/AgCl. Some of the soliton walls of the Au reconstruction remain. (b) At −0.051 V versus Ag/AgCl, after stripping the Au−Cd alloy nanowires from the surface. Scan size is 70 × 70 nm^2.

structures. From Figure 2, it is evident that the soliton walls and the hcp regions between have on average a higher potential energy than the fcc regions, facilitating alloy nanowire formation.